EXPLORING MOISTURE FLUX AVAILABILITY ABOVE THE SEA FOR ATMOSPHERIC WATER GENERATION

Afeefa Rahman[1, 2], Siam Alam*[3]

[1] *Ph.D. Candidate, University of Illinois at Urbana–Champaign, USA, e-mail: afeefar2@illinois.edu*
[2] *Assistant Professor, Bangladesh University of Engineering and Technology, Bangladesh, e-mail: afeefa@wre.buet.ac.bd*
[3] *Research Consultant, Center for Environmental and Geographic Information Services, Bangladesh, e-mail: siam94015@gmail.com*

***Corresponding Author**

ABSTRACT

In this study, we delve into the moisture flux availability over the sea surface and its potential for contributing to the production capacity of atmospheric water generation systems. Understanding that a higher moisture flux availability in the atmosphere directly translates to a greater reservoir of water vapor accessible for extraction and condensation, we embark on an investigation centered on seas and gulfs across the Middle East, parts of North Africa, and western Asia – regions currently grappling with elevated freshwater stress. Our methodology uses ERA-5 data from 2009 to 2019, encompassing key meteorological variables at the near-surface level of the atmosphere. Employing the Monin-Obukhov similarity theory, we extract the required variables for different atmospheric stability conditions, enabling us to compute the horizontal moisture flux within the surface sublayer above the selected seas and gulfs. Our findings, derived from a comprehensive analysis of ten years of daily data, reveal distinct seasonal patterns. During December, January, and February, the selected seas and gulfs experience comparatively lower moisture flux levels, often falling below the threshold of 0.07 $kg/m^2 \cdot s$. In stark contrast, the summer months of June, July, and August witness the highest moisture flux, with particularly robust concentrations detected in the deep Arabian and Red Sea. We delineate a 50-kilometer-wide zone from the shoreline of each sea and gulf to calculate the zonal mean moisture flux. This detailed analysis unearths regions with notably heightened moisture flux availability. Notably, the Arabian Sea, Bay of Bengal, Red Sea, and Gulf of Aden emerge as strong contenders, boasting significantly higher moisture flux than other study locations. Our study outcomes bear significant implications for regional water resource management. By pinpointing areas with abundant atmospheric moisture above the sea, we lay the foundation for potential solutions to alleviate freshwater scarcity through atmospheric moisture harvesting.

Keywords: *Moisture Flux, ERA-5, Monin-Obukhov Similarity Theory, Atmospheric Moisture Harvesting, Freshwater Scarcity*

1. INTRODUCTION

Around one billion people in the world currently lack adequate fresh water for their livelihood (Lindblom & Nordell, 2006), and prediction says half of the world's total population will face acute freshwater scarcity by 2025 (Mekonnen & Hoekstra, 2016). Ever-growing global population, urbanization, and extreme climatic events (drought, flood, storm surge) brought by natural and anthropogenic drivers might induce even more pressure on limited freshwater resources making the issue of freshwater scarcity one of the most critical ones for the current world (Salehi et al., 2020; Wu et al., 2020).

With a noble aim to overcome freshwater scarcity and eliminate the constraint of limited water resources, the research community put several efforts into developing evolving strategies. The solutions available in today's world to solve the freshwater crisis include seawater desalination, rainwater harvesting, wastewater treatment, sewage recycling, and water production from humid air (Atmospheric moisture harvesting) and fog harvesting (Wu et al., 2020). However, the available technologies for producing freshwater have a unique set of confines. For instance, energy consumption in the desalination, chemical treatment, and recycling of saline and wastewater is pretty high, and the production efficiency of the rainwater harvesting system and dew harvesting is quite low. Thus, investigating emerging technologies for improved alternatives to ensure energy-efficient freshwater production is still a prime need.

Atmospheric moisture harvesting refers to technologies that extract moisture from the air and convert it into freshwater, typically by involving condensation or other techniques to condense the water vapor within the collected airmass. It has the potential to provide a sustainable and decentralized source of freshwater for areas where traditional water sources are scarce or overexploited. The humid atmosphere can be considered a potential source of water production as records show that the largest reserve of water is available in the atmosphere (Salehi et al., 2020), although in vapor form. Some atmospheric, mechanical, and chemical approaches are known to produce fresh water from the thin-moist layer of the atmosphere. Condensation of humid air within a condensation tower or solar chimney (Kashiwa & Kashiwa, 2008; Ming et al., 2017; Wu et al., 2020), Extraction of air and condensation by using vapor pressure compression cycle (Bolsinger & Ralphs, 2019; Vinay et al., 2018), use of desiccant materials for adsorption and absorption of moisture within the humid air (Liu et al., 2017), the capture of humid air and condensation in the underground region (Alnaser & Barakat, 2000; Lindblom & Nordell, 2006), water from fog harvesting (Morichi et al., 2018) are the available approaches to be mentioned. The diverse techniques employed for atmospheric water harvesting can be categorized into two primary groups: condensation and sorption, as illustrated in Figure 1. Nonetheless, these technologies' efficiency in producing water from humid air is indeed a critical issue to consider.

Most of the available atmospheric moisture harvesting approaches are mostly theoretical or experimental on a tiny scale, demanding more effort to validate the idea and number estimates. For instance, (Wu et al., 2020) proposed a modified solar chimney for large-scale freshwater production from the humid atmosphere where a 1000m tall solar chimney can theoretically be capable of producing 6×10^{10}10 kg of water per year. The number estimate is the output from a mathematical model and does not have any experimental validation yet. Besides, the production capacity of many of the available approaches is relatively low. For example, (Lindblom & Nordell, 2006) suggested underground condensation of the humid atmosphere in which the water production rate is 3 kg/ m^2.day. The lower production capacity is attributed to the fact that those theories talk about the land-based setup of the moisture harvesting system. Whereas the coastal atmosphere and the atmosphere above oceans should be more suitable for atmospheric moisture harvesting since the air of these areas is nearly saturated throughout the year (Ahrestani et al., 2023).

Despite the proximity to the vast expanse of the ocean and humid atmospheres, the pressing issue of freshwater scarcity persists in many coastal regions worldwide. Notably, the Middle East, North Africa (MENA), and parts of Western Asia stand as glaring examples of the most water-stressed regions on Earth (WRI, 2017). This context has sparked our interest in estimating moisture flux in the surface sublayer of the atmosphere above seas and gulfs. By focusing on the potential of moisture harvesting from the atmosphere above the sea and gulf areas in the Middle East, parts of North Africa, and Western Asia, we aim to address a critical gap in the current understanding of water resource management in these regions. The outcome of this study holds far-reaching implications, extending beyond the realms of innovative technology. If successful, moisture harvesting from these specific atmospheric zones could signify a paradigm shift in addressing freshwater scarcity, offering a sustainable solution to regions grappling with chronic water shortages. By delving into the untapped potential atmosphere above seas and gulfs, we aspire not only to advance scientific knowledge but also to contribute to the development of practical, scalable strategies for mitigating water stress in some of the world's most vulnerable areas.

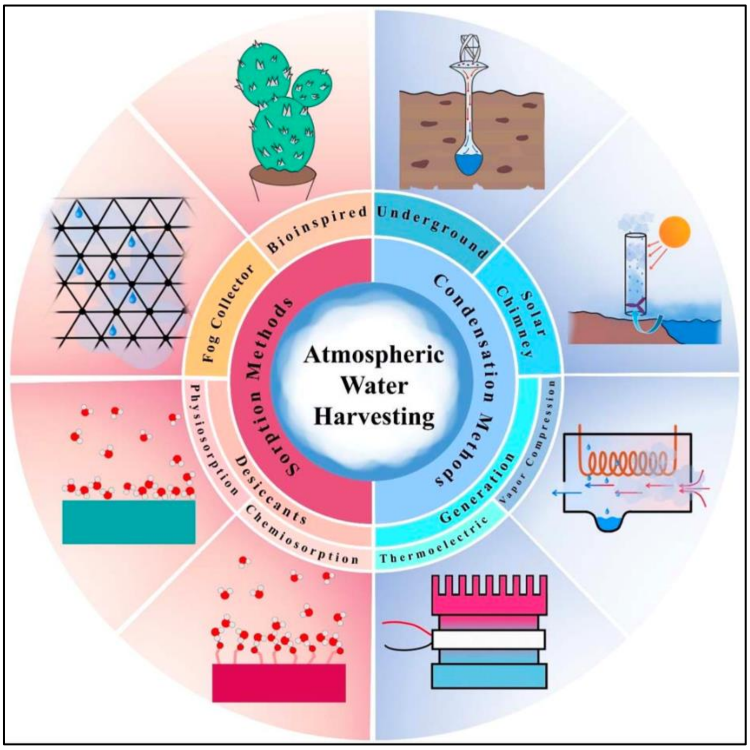

Figure 1: Diverse Techniques for Atmospheric Water Harvesting

2. METHODOLOGY

2.1 Study Area and Data Collection

In this study, we aim to analyze and compare the moisture flux availability in the surface sublayer of the atmosphere above the sea to establish the coastal atmosphere's superiority as the source of moisture for a harvesting system. In this regard, a zone with higher freshwater stress and access to seas and gulfs would be the most reasonable choice. Estimates show that in the Middle East, North Africa, and Western Asia, the total water withdrawal and usage is more than 80% of the total freshwater availability putting stress on the existing freshwater sources. This is why a domain, including the Middle East, North Africa, and Western Asian countries, has been proposed as the study location. As depicted in Figure 2, our study area includes detailed topographic features. This region is characterized by the substantial landmass of India in Western Asia and the prominent presence of Saudi Arabia in the Arabian Peninsula. Surrounding these landmasses are thirteen major water bodies, including the Mediterranean Sea, Aegean Sea, Sea of Marmara, and the Black Sea in the northwest, the Gulf of Aqaba and Gulf of Suez in the West, the Persian Gulf and the Gulf of Oman in the Northeast, the Arabian Sea, Laccadive Sea, and Bay of Bengal in the southeast, the Red Sea in the Southwest, and the Gulf of Aden in the south. For performing the analyses, data on seven micro-meteorological variables for the time range 2009-2019 have been collected from ERA-5 as represented in Table 1. These datasets have been used to calculate the moisture flux in the surface sublayer of the atmosphere above the sea surface of the study domain.

Table 1: Data Type and Variables

Variables	Data type	Collection period
10m u and v component of wind Friction velocity 2m temperature and dewpoint temperature Air pressure Air density at 2m Instantaneous Surface sensible heat flux Instantaneous water vapor flux	ERA-5 dataset on single levels with spatial resolution of 27 km by 27 km	2009-2019

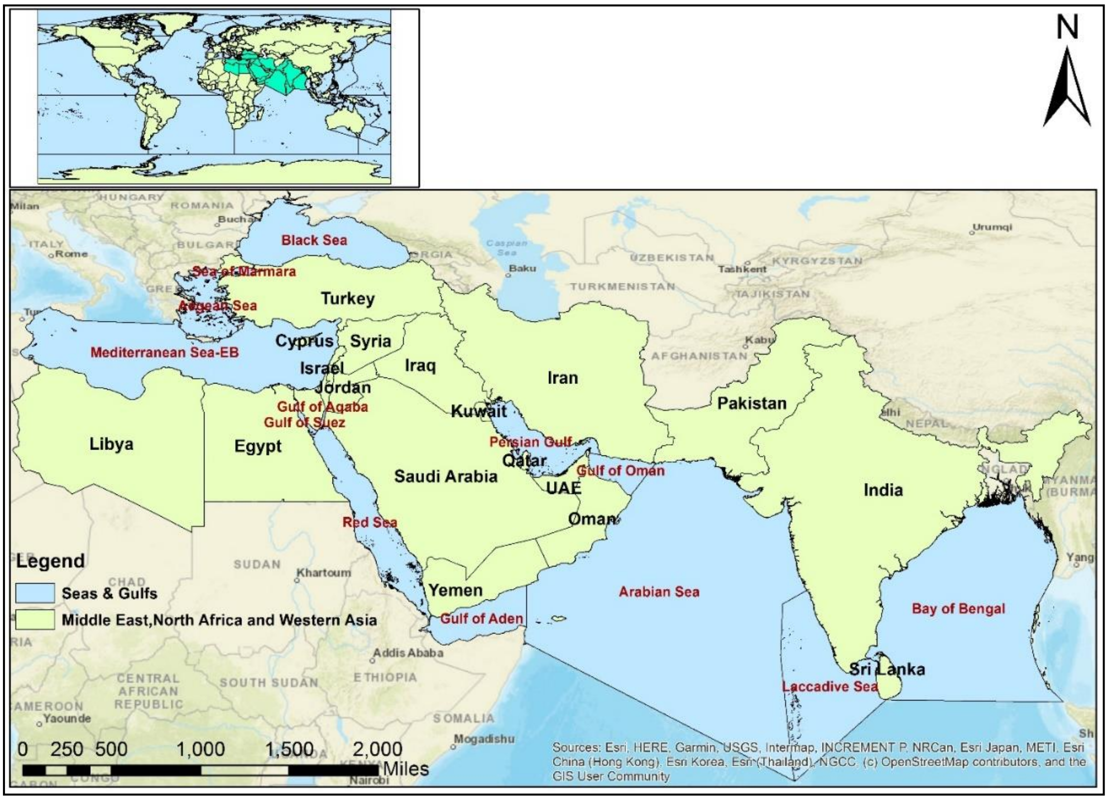

Figure 2: Locations of the Study Domain

2.2 Governing Equations for the Calculation of Moisture Flux

In delving into the mechanics of moisture flux calculation, a fundamental understanding of the governing equations is paramount. We start with the ERA-5 data for the near-surface variables that provide air pressure and density at 2m height above the surface. With the surface information of pressure and density, the values for these corresponding variables at 10m are calculated using Poisson's equation and the ideal gas law, as shown in equations 1 and 2.

$$P_a = P_s \left(\frac{T_a}{T_s}\right)^{\frac{C_p}{R_a}} \tag{1}$$

where, $R_a = R_d(1+0.611q)$; P_s = Near-surface air pressure; Ts = near-surface temperature

$$\rho_a = \frac{P_a}{R_a T_a} \tag{2}$$

The chosen data category within ERA-5, unfortunately, lacks information on specific humidity. To address this, specific humidity at 2 meters above the surface is derived utilizing the Clausius-Clapeyron equation, which hinges on actual vapor pressure. We compute the actual vapor pressure from the dew point temperature, as shown in Equation 3. The relationship between specific humidity and actual vapor pressure is intricately defined in Equation 4, forming a pivotal bridge between the available data and the specific humidity variable which is essential for our comprehensive analysis.

$$e = 611 \times \exp\left[\frac{L}{R_v}\left(\frac{1}{273.15} - \frac{1}{T_d}\right)\right] \tag{3}$$

$$q = \frac{0.622e}{\mathrm{P_a} - 0.378\,e} \tag{4}$$

Where, e = actual vapor pressure; L_v = Latent heat of vaporization; T_d = Dew point temperature, and R_v = 461.5 J/kg/K.

The mean profile of temperature, wind speed, and specific humidity are considered as the logarithmic function of height above the surface. These three variables at the desired height are obtained from the flux profile relationship invoked from the Monin-Obukhov similarity theory by applying dimensional analysis (Brutsaert, 1982). For instance, the expression for the temperature is-

$$T_2 = T_1 - \frac{H}{a_h k u_* \rho C_p}\left[ln\frac{z_2 - d_o}{z_1 - d_o} - \Psi_h\left(\frac{z_2}{L}\right) + \Psi_h\left(\frac{z_1}{L}\right)\right] \tag{5}$$

Where, T_1 is the temperature at 2 m height above the surface, H = instantaneous surface sensible heat flux (J/m^{2}s), Z_1 = 2 m, and Ψ_h is the profile function for temperature; varies depending on the stability of the atmospheric layer (Surface sublayer in our case).

For Neutral condition,
$\Psi_h = 0$

For Stable Condition,
$\Psi_h = -\frac{5z}{L}$ for $0 < \frac{z}{L} \leq 1$;
$\Psi_h = -5$ for $\frac{z}{L} > 1$;

For Unstable condition,
$\Psi_h = 2\ ln\left[\frac{(1+x^2)}{2}\right]$
Where, $x = \left(1 - 16\frac{z}{L}\right)^{-0.5}$ (6)

The stability of the atmospheric layer is obtained from Obukhov's Stability length, L as shown in Equation

$$L = -\frac{{u_*}^3 \rho_a}{a_h k\left[\left(\frac{H}{T_a C_p}\right) + 0.61E\right]} \tag{7}$$

Where, E = Water vapor/instantaneous moisture flux (kg/m^{2}s); H = instantaneous sensible heat flux (J/m^{2}s); T_a is the atmospheric temperature at 2 m, u_* is the friction velocity and ρ_a is the air density at 2m height. There are five conditions of atmospheric stability according to Obukhov's Length; if the L is between 0 to 200, the condition is termed as very stable; when it is between 200 to 1000, the atmosphere is stable; above 1000, the length represents a neutral condition of atmosphere, a negative value of the Obukhov length means the unstable and very unstable atmospheric conditions. A similar set of equations representing the flux profile relationship for specific humidity and wind speed are shown in the equation from 8 to 13.

$$q_2 = q_1 - \frac{E}{a_v k u_* \rho}\left[ln\frac{z_2 - d_o}{z_1 - d_o} - \Psi_v\left(\frac{z_2}{L}\right) + \Psi_v\left(\frac{z_1}{L}\right)\right] \tag{8}$$

Where Ψ_v is the profile function for water vapor that varies depending on the stability of the atmospheric layer.

For Neutral condition,
$\Psi_v=0$

For Stable Condition,
$\Psi_v = -\frac{5z}{L}$ for $0<\frac{z}{L} \leq 1$;
$\Psi_v = -5$ for $\frac{z}{L} > 1$;

For Unstable condition,
$\Psi_v = 2\ ln\left[\frac{(1+x^2)}{2}\right]$
Where, $x = \left(1 - 16\frac{z}{L}\right)^{-0.5}$

(9)

$$u_2 = u_1 + \frac{u_*}{k}\left[ln\frac{z_2 - d_o}{z_1 - d_o} - \Psi_m\left(\frac{z_2}{L}\right) + \Psi_m\left(\frac{z_1}{L}\right)\right] \tag{10}$$

Where Ψ_m is the profile function for wind.

For Neutral condition,
$\Psi_m=0$

For Stable Condition,
$\Psi_m = -\frac{5z}{L}$ for $0<\frac{z}{L} \leq 1$;
$\Psi_m = -5$ for $\frac{z}{L} > 1$;

For Unstable condition,
$\Psi_m = 2\,ln\left[\frac{(1+x)}{2}\right] + ln\left[\frac{(1+x^2)}{2}\right]$
$-2tan^{-1}x + \frac{\pi}{2}$
Where, $x = \left(1 - 16\frac{z}{L}\right)^{-0.25}$

(11)

Once we have the required meteorological variables at the 10m height above the surface, the moisture flux estimate at that level is obtained from equation eight, which represents the amount of moisture transported per unit vertical area in the atmospheric layer per unit time. Moisture flux transport is hereby described in terms of the specific humidity (q) and the wind vector.

Moisture Flux for a layer $= \overline{\rho_a qU}$ in kg of water/m^2s (12)

The derived moisture flux, as delineated in Equation 12, is subsequently scaled by the total seconds in a day. This operation yields the daily moisture flow per unit area. By cumulating these mean daily moisture flows over the course of the years, we arrive at the comprehensive yearly mean moisture availability within the near-surface atmosphere above our designated study locations. This calculated parameter serves as a crucial metric in assessing the long-term moisture dynamics and forms a foundation for understanding the sustainable potential for atmospheric water harvesting in the selected regions. Figure 3 is a sample box plot showing the monthly mean moisture flux calculated from 10-year data in the Persian Gulf near Doha Qatar. After obtaining the moisture flux estimate for all the grids in the study domain, an area with a 50 km width from the shoreline has been delineated for all thirteen sea and gulf areas to compute the zonal average of the moisture flux. Variation of moisture flux along the 50 km width in the Arabian Sea is shown in Figure 4. The simplistic flow diagram of the major steps of the project is shown in Figure 5.

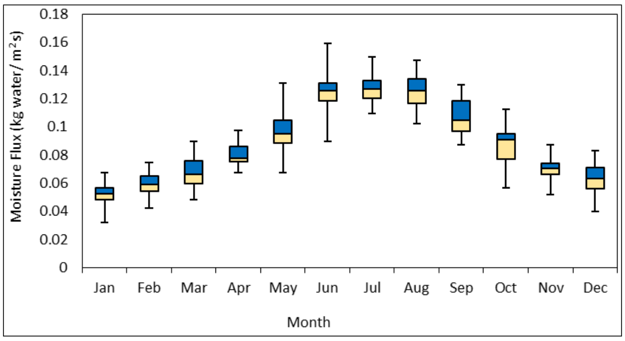

Figure 3: Monthly Mean moisture flux in a 27 km by 27 km grid in the Persian Gulf

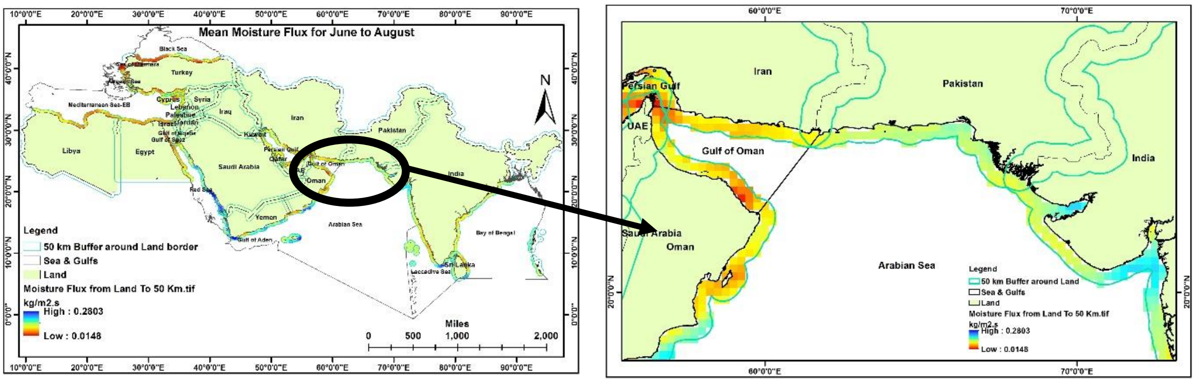

Figure 4: Variation of Moisture Flux along the 50 Km width in the Arabian Sea

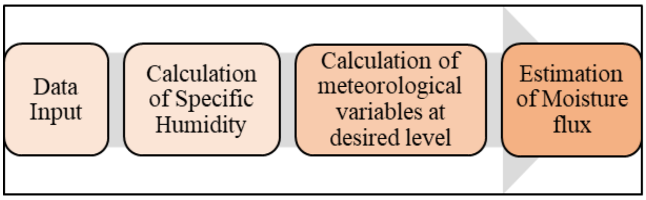

Figure 5: Methodological framework of this project.

3. RESULTS AND DISCUSSION

3.1 Seasonal Variation of Moisture Flux Across the Study Domain

Generally, the moisture flux in the atmosphere exhibits an increasing trend from land toward the shoreline and a discernible trend as one moves from the shoreline toward the deep sea. Land surfaces typically heat up and cool down more quickly than water, leading to variations in temperature that affect the air's capacity to hold moisture. Also, the land surface has a very limited capacity to supply humidity into the overlaying atmosphere, depending on the soil moisture and the water source. On the other hand, near the shoreline, where land and sea meet, the moisture flux is often higher, which is influenced by several factors, including the temperature contrast between the land and sea, the availability of moisture from the water surface, and the coastal geography. Interestingly, over the deep sea, where water covers a vast expanse, the moisture flux tends to be more uniform. The large water body provides a relatively constant source of moisture, contributing to a more stable atmospheric moisture content. It's important to note that local variations, such as wind patterns, geographical features, and seasonal changes, can influence this general trend (Islam et al., 2013; Luo et al., 2015).

To comprehensively assess these fluctuations, mean moisture flux values were computed for four distinct seasonal categories: December to February (winter), March to May (spring), June to August (summer), and September to November (autumn). Figure 6(a) to (d) illustrates a noteworthy finding: the lowest mean moisture flux occurs during the winter months (December to February). During this period, a predominant portion of the seas and gulfs within the study area experienced moisture flux values consistently below 0.04 kg/m²s. Notably, the deep Arabian Sea, Gulf of Aden, Red Sea, and Bay of Bengal exhibit slightly elevated mean moisture flux, ranging from 0.04 to 0.07 kg/m²s. During the period, a significant part of the Persian Gulf, Mediterranean Sea, Black Sea, and Arabian Sea near coastal Pakistan experienced moisture flux below 0.01 kg/m²s. Generally, winter months are characterized by lower atmospheric temperatures which creates a reduced capacity for the air to hold moisture, resulting in lower moisture flux. The limited temperature differential between the land and sea contributes to decreased atmospheric moisture transport. Atmospheric Stability and oceanic influence are also important for such seasonal trends.

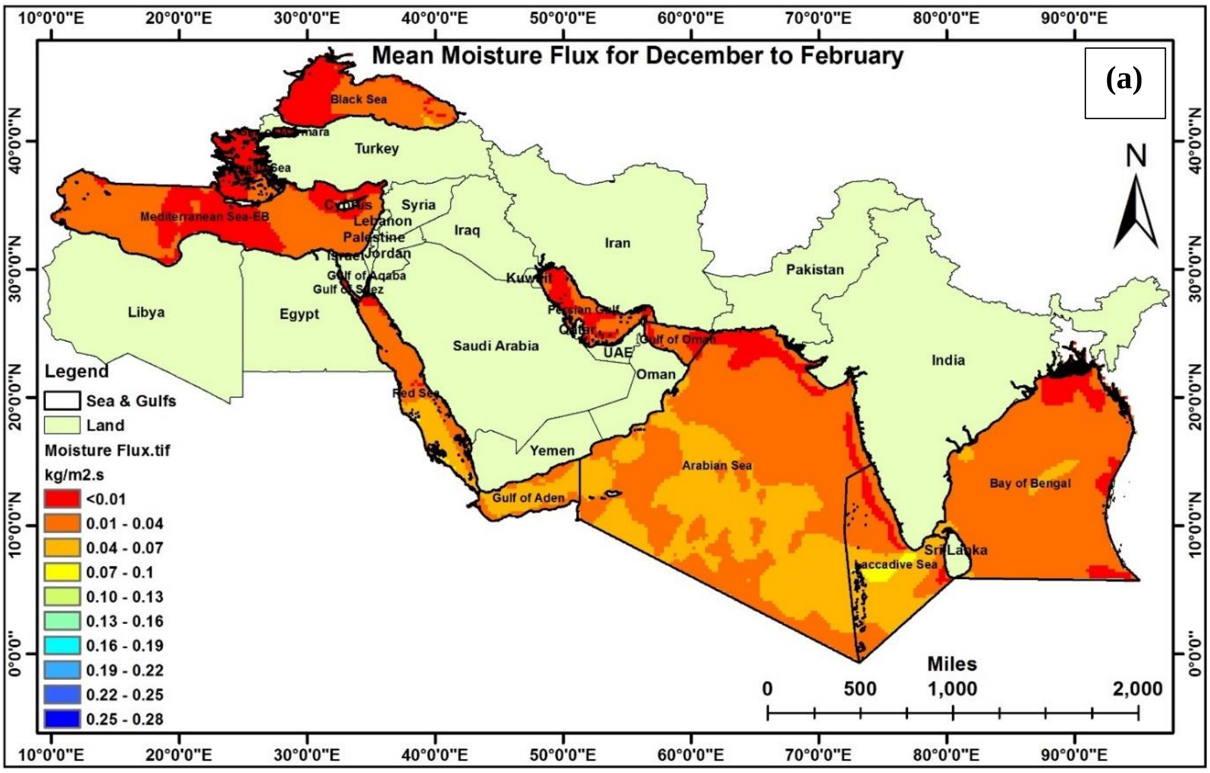

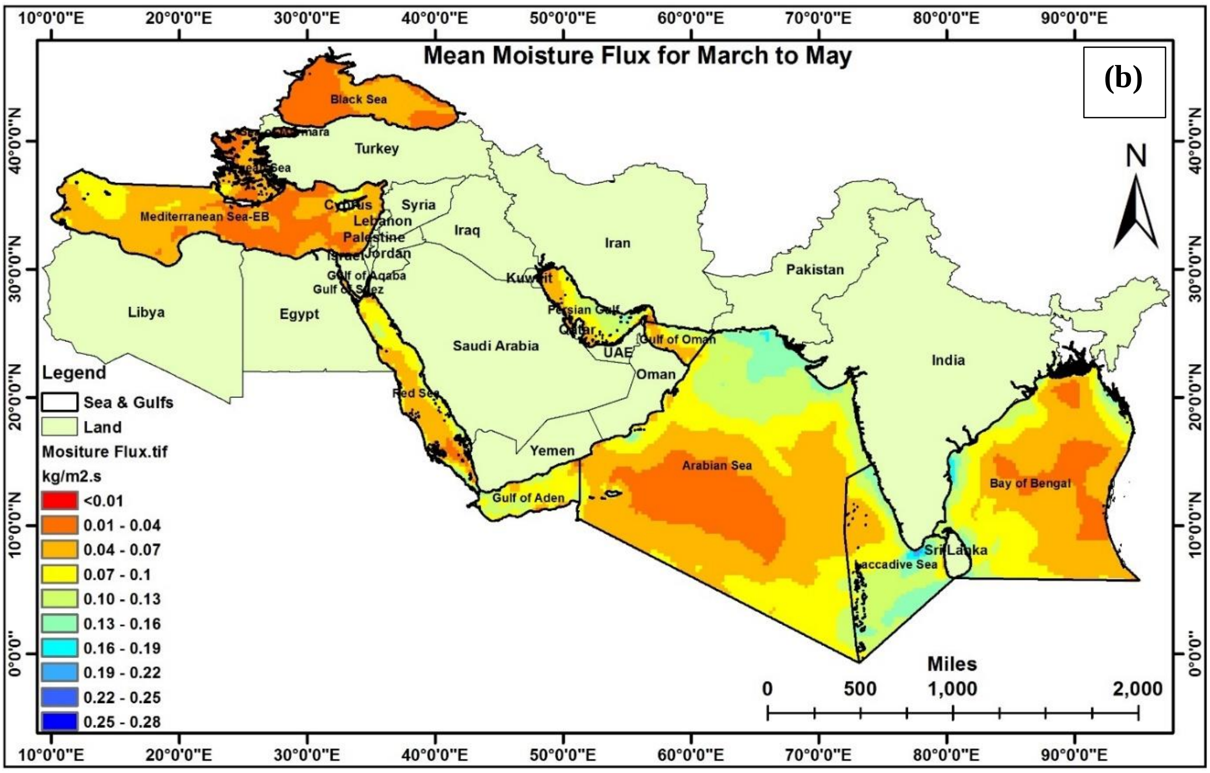
Mean Moisture Flux for March to May
(b)
Legend
Sea & Gulfs
Land
Mositure Flux.tif
kg/m2.s
<0.01
0.01 - 0.04
0.04 - 0.07
0.07 - 0.1
0.10 - 0.13
0.13 - 0.16
0.16 - 0.19
0.19 - 0.22
0.22 - 0.25
0.25 - 0.28
Miles
0 500 1,000 2,000

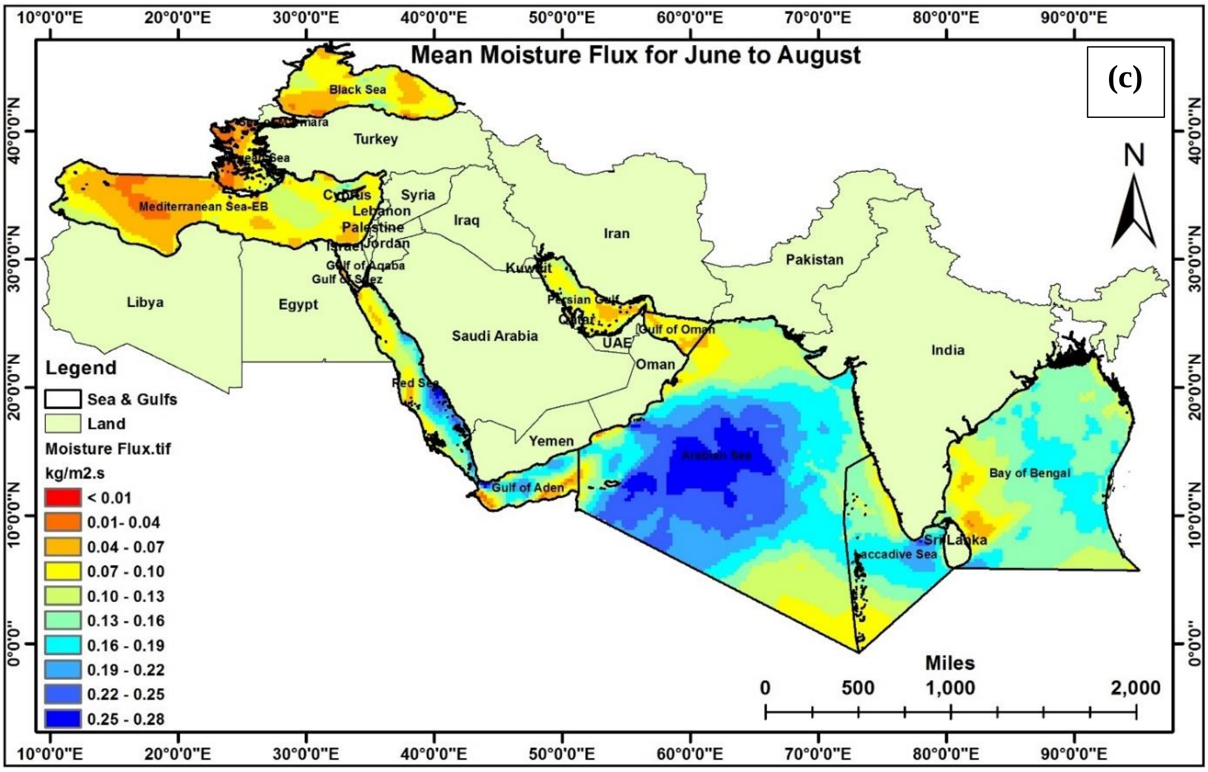
Mean Moisture Flux for June to August
(c)
Legend
Sea & Gulfs
Land
Moisture Flux.tif
kg/m2.s
< 0.01
0.01- 0.04
0.04 - 0.07
0.07 - 0.10
0.10 - 0.13
0.13 - 0.16
0.16 - 0.19
0.19 - 0.22
0.22 - 0.25
0.25 - 0.28
Miles
0 500 1,000 2,000

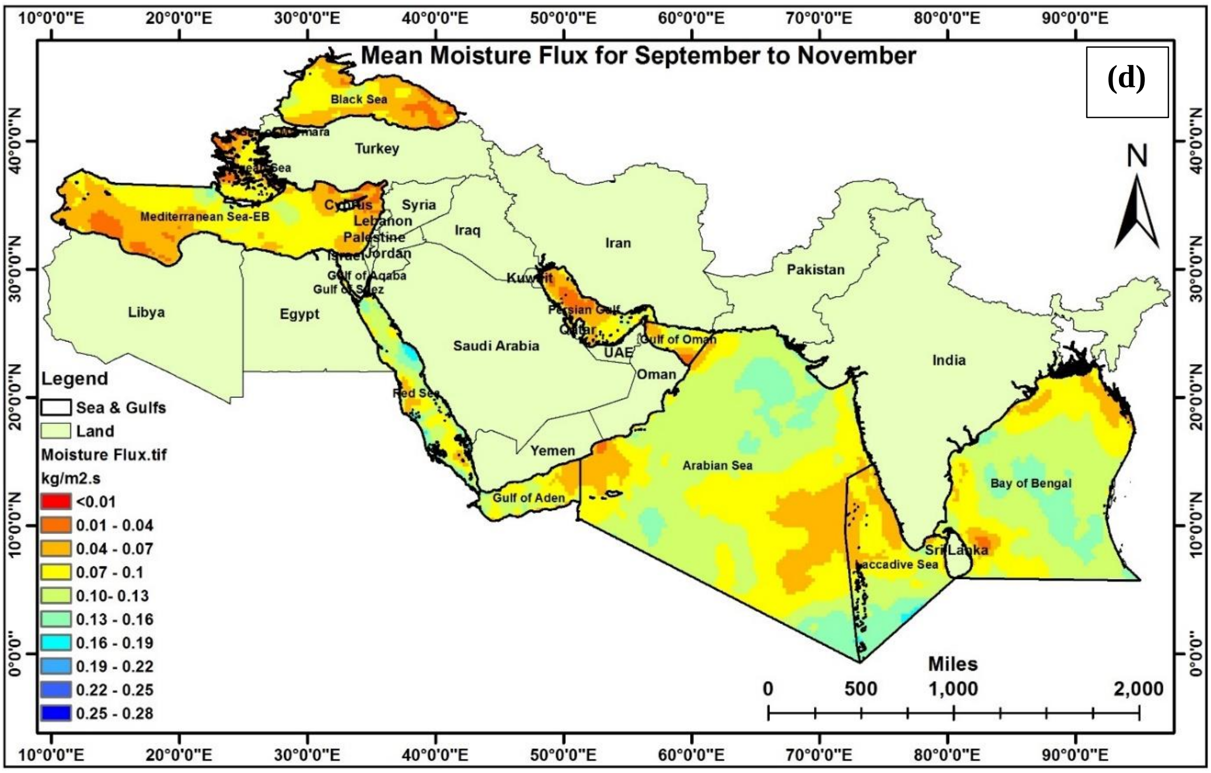

Figure 6: Mean Moisture Flux in the Study Domain (a) December to February (b)March to May (c)June to August (d) September to November

Winter is often associated with increased atmospheric stability, reducing vertical motion and consequently impeding the upward transport of moisture. This stability can contribute to lower moisture flux values observed during this season. The slightly elevated mean moisture flux observed in specific areas, such as the deep Arabian Sea, Gulf of Aden, Red Sea, and Bay of Bengal, could be attributed to localized oceanic processes. These regions may exhibit unique oceanic-atmospheric interactions that contribute to a more moderate decline in moisture flux during winter.

During the months of March, April, and May, moisture flux varied from 0.04 to 0.16 kg/m^{2}s with higher values near a part of India and Sri Lanka in the Laccadive Sea and coastal Pakistan in the Arabian Sea even though a part of the Deep Arabian Sea and Bay of Bengal still experience lower moisture flux below 0.01 kg/m^{2}s. Moisture flux increases as we move along the months of the year. Moisture flux is higher during the months from June to August and September to November. We see pockets of very high moisture flux in the deep Arabian Sea, Laccadive Sea, and Red Sea. From June to August, in most parts of the study domain, moisture flux is around 0.04 to 0.19 kg/m^{2}s. As a spatial comparison, the Black Sea, the Aegean Sea, the Mediterranean Sea, the Gulf of Aqaba, and the Gulf of Suez experience lower moisture flux than the Bay of Bengal, Arabian Sea, Gulf of Aden, Gulf of Oman, and red Sea. Higher moisture flux observed during the summer months can be attributed to the increased solar flux induced by higher air temperature, greater water vapor, and sensible heat flux during the summer months. The greater availability of solar energy during this period intensifies the sensible heat flux, fostering a conducive environment for enhanced moisture transport. The increased water vapor content during the summer months contributes to a more buoyant atmosphere, promoting upward motion and facilitating higher moisture flux. Additionally, heightened sensible heat flux during this period enhances the evaporation process, further augmenting moisture transport. Here we formulated the moisture flux in terms of the specific humidity and wind speed. Both climatic variables play a vital role in shaping various forms of atmospheric energy, particularly the latent heat transport from the tropics to mid-latitudes. Higher moisture flux might be linked with the increased latent heat transport to the zone as well. The observed patterns provide valuable insights into the temporal dynamics of moisture flux, offering a foundation for developing targeted strategies to optimize water harvesting technologies in alignment with seasonal conditions.

3.2 Identifying the Zones with Significant Moisture Flux Availability

Zonal mean moisture flux representative for the whole year for all thirteen seas and gulfs have been calculated from a delineated sea area with 50 km width and compared. The bar chart, as shown in Figure 7, shows the comparison. Strikingly, the Gulf of Aden, Arabian Sea, Bay of Bengal, and the Red Sea emerge as key contributors, consistently supplying higher moisture flux compared to the other seas and gulfs. This observation underscores the inherent climatic advantages of certain regions, favoring countries such as Yemen, Oman, Egypt, Saudi Arabia, Pakistan, and India with notably higher moisture flux availability. The geographical distribution of elevated moisture flux is indicative of a natural predisposition, portraying these nations as better endowed in terms of atmospheric moisture content. The implications of these findings are noteworthy, particularly in the context of implementing moisture harvesting systems. The conclusion drawn is that, if the objective is to establish a moisture harvesting system in proximity to selected locations among these thirteen major water bodies, priority should be given to areas characterized by higher moisture flux. The strategic selection of these locations not only capitalizes on the natural abundance of atmospheric moisture but also aligns with the overarching goal of optimizing the efficiency and effectiveness of moisture harvesting initiatives in these geographically privileged regions.

The findings presented in Table 2 offer a comprehensive overview of the yearly mean moisture flux across all water bodies within our study domain. Notably, the data reveals a magnitude ranging from 10^6 to 10^7, signifying the substantial amount of moisture available per square meter vertical area in the atmospheric layer near the sea surface. This variability underscores the potential viability of utilizing this atmospheric layer as a dependable source for moisture harvesting in freshwater production.

To illustrate the practical implications of these findings, let us consider a hypothetical scenario. If a moisture harvesting setup were strategically deployed above seas and gulfs within our study area—with a harvesting system having efficiency for the collection of air and condensation of air of about 10% and operational 24 hours a day—the resulting water production from the airmass collected per square meter of the atmospheric area would range from 10^5 to 10^6. Translating this into practical terms, assuming a per capita water consumption of 340 Liters for coastal communities, the harvesting system of such a tiny scale has the potential to sustainably provide for approximately 6-8 individuals throughout the entire year with a potential for serving way more people if we scale up the harvesting system. These results underscore the promising feasibility of implementing moisture harvesting systems as a sustainable solution to freshwater scarcity in coastal regions. The ability to support a significant number of individuals emphasizes the broader societal impact of harnessing atmospheric moisture, paving the way for transformative water resource management practices in water-stressed coastal communities.

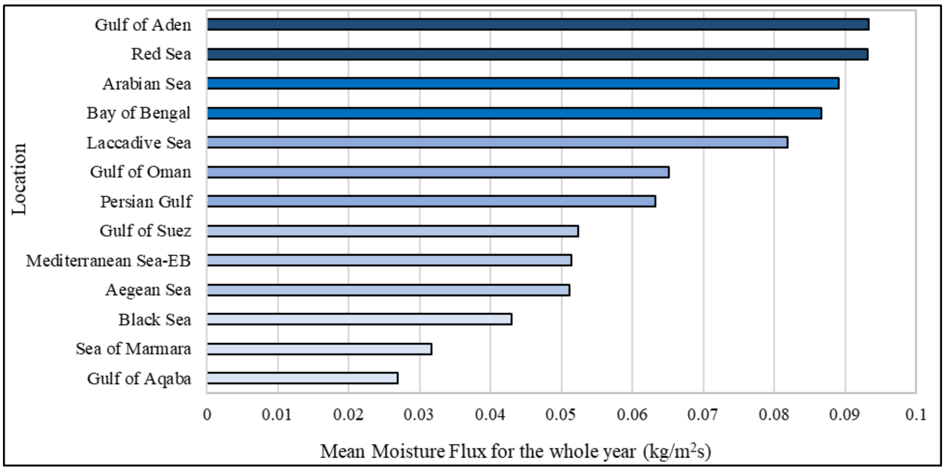

Figure 7: Adsorbed Arsenic Concentration for 1D Numerical Simulation and Experimental Observation

Table 2: Yearly Mean Moisture Flux

Location	Yearly Mean Moisture Flow (kg/m^{2}year)
Gulf of Aden	2940183
Red Sea	2936316
Arabian Sea	2807737
Bay of Bengal	2730615
Laccadive Sea	2581088
Gulf of Oman	2052844
Persian Gulf	1992635
Gulf of Suez	1650889
Mediterranean Sea-EB	1618728
Aegean Sea	1611478
Black Sea	1354177
Sea of Marmara	998599
Gulf of Aqaba	847062

4. CONCLUSIONS

The conventional reliance on traditional water sources such as rivers and aquifers often falls short of meeting the escalating demand driven by population growth and industrialization. In response to this challenge, the concept of atmospheric water generation emerges as a promising alternative, offering a potential solution to alleviate freshwater stress in these areas. By harnessing the humidity present in the atmosphere, technologies designed for atmospheric water generation can provide a decentralized and sustainable source of freshwater. This method not only reduces the environmental impact associated with traditional water extraction but also ensures a diversified water supply that enhances resilience in the face of climate change. Particularly advantageous for remote or isolated coastal communities, atmospheric water generation stands as a beacon of hope, addressing water security concerns and ushering in a new era of innovative and accessible freshwater solutions for regions grappling with the imminent threat of freshwater scarcity. With such perspective, the current endeavor investigated the seasonal variation of moisture flux above the near-sea surface layer of the gulfs and seas around the Middle East, parts of North Africa, and Western Asian countries. The study result depicts the temporal variability of the moisture flux at the selected locations, highlighting prominent seasonal variability. The Gulf of Aden, Arabian Sea, Bay of Bengal, and Red Sea supply maximum moisture flux among the selected seas, and gulfs are more suitable for atmospheric moisture harvesting. The study findings reveal the possibility of using the atmospheric layer above the sea, gulfs, and major water bodies as a potential freshwater production source since significant water reserves are available in the atmosphere, although in vapor form. The idea can be implemented for regions with high freshwater stress and access to oceanic regions to harvest moisture, preferably during the summer months from June to August. The significance of our research lies not only in its potential to revolutionize water resource management but also in its broader impact on fostering resilience and sustainability in the face of a growing global water crisis.

REFERENCES

Alnaser, W. E., & Barakat, A. (2000). Use of condensed water vapour from the atmosphere for irrigation in Bahrain. *Applied Energy*, *65*(1–4), 3–18.

Ahrestani, Z., Sadeghzadeh, S., & Emrooz, H. B. M. (2023). An overview of atmospheric water harvesting methods, the inevitable path of the future in water supply. RSC advances, 13(15), 10273-10307.

Bolsinger, C. C., & Ralphs, S. P. (2019). Atmospheric Water Generation. *Bolsinger, CC, & Ralphs, SP*, 335.

Islam, S. T., Huszczynski, S. M., Nugent, T., Gold, A. C., & Lam, J. S. (2013). Conserved-residue mutations in Wzy affect O-antigen polymerization and Wzz-mediated chain-length regulation in Pseudomonas aeruginosa PAO1. Scientific Reports, 3(1), 3441.

Kashiwa, B. A., & Kashiwa, C. B. (2008). The solar cyclone: A solar chimney for harvesting atmospheric water. *Energy*, *33*(2), 331–339.

Lindblom, J., & Nordell, B. (2006). Water production by underground condensation of humid air. *Desalination*, *189*(1–3), 248–260.

Liu, S., He, W., Hu, D., Lv, S., Chen, D., Wu, X., Xu, F., & Li, S. (2017). Experimental analysis of a portable atmospheric water generator by thermoelectric cooling method. *Energy Procedia*, *142*, 1609–1614.

Luo, T., Young, R., & Reig, P. (2015). Aqueduct projected water stress country rankings. Technical Note, 16.

Mekonnen, M. M., & Hoekstra, A. Y. (2016). Four billion people facing severe water scarcity. *Science Advances*, *2*(2), e1500323.

Ming, T., Gong, T., de Richter, R. K., Wu, Y., & Liu, W. (2017). A moist air condensing device for sustainable energy production and water generation. *Energy Conversion and Management*, *138*, 638–650.

Morichi, G., Calixto, L. B., & Zanelli, A. (2018). Novel applications for fog water harvesting. *Journal of Geoscience and Environment Protection*, *6*(3), 26–36.

Salehi, A. A., Ghannadi-Maragheh, M., Torab-Mostaedi, M., Torkaman, R., & Asadollahzadeh, M. (2020). A review on the water-energy nexus for drinking water production from humid air. *Renewable and Sustainable Energy Reviews*, *120*, 109627.

Vinay, M. V, Suman, A., & Shadakshari, R. (2018). Dehumidification of atmospheric air for water production. *Int. J. Innov. Res. Sci. Eng. Technol*, *7*, 3808–3813.

WRI. (2017). Forging Ahead. World Resources Institute Annual Report, 23(8), 3–3. https://doi.org/10.1002/pfi.4150230804

Wu, Y., Ming, T., de Richter, R., Höffer, R., & Niemann, H.-J. (2020). Large-scale freshwater generation from the humid air using the modified solar chimney. *Renewable Energy*, *146*, 1325–1336.